International Journal on Engineering, Science and Technology
Volume 4, Issue 1, 2022 ISSN: 2642-4088

Multi-Objective and Robust Design of a Semi-Active Suspension System

Muhammad Ali Khan
Marshall University, USA

Yousef Sardahi
Marshall University, USA, sardahi@marshall.edu

Carlos Ignacio Hernández Castellanos
Instituto de Investigaciones en Matemáticas Aplicadas y en Sistemas, Universidad Nacional Autónoma de México, USA

Abstract This paper presents a robust multi-objective optimal design (RMOP) of a passenger car with a semi-active suspension system. The mean-effective values of the root mean square of the passenger's head acceleration, suspension travel, and tire deflection are considered as design objectives. The passive components of the suspension and the design details of the Linear Quadratic Regulator (LQR) algorithm are used as design parameters. During the design, global sensitivity analysis is carried out using the Fourier Amplitude Sensitivity Test (FAST) to specify the elements of the model that can highly alter the design objectives. The mass of the passenger's head and upper body, the mass of the passenger's lower body and cushion, passenger and cushion's elastic properties, and the sprung mass of the vehicle are selected for the sensitivity analysis. Results show that the design criteria are very sensitive to the variations in the sprung mass of the vehicle as compared to the other parameters. As a result, the variations in this parameter and passive elements of the suspension system are considered. Constraints are applied on the objectives in compliance with the requirements of ISO 2631-1 on the design of car suspension systems. The optimization problem is solved by the NSGA-II (non-dominated sorting genetic algorithm II) and robust Pareto front and set are obtained. The Pareto set includes multiple design options from which the decision-maker can choose to implement. Responses of the passenger's head acceleration, suspension travel, and tire deflection show that the robust multi-objective design algorithm (RMOA) is very effective and guarantees less sensitivity to the suspension passive elements.

Keywords: multi-objective optimization, robust and optimal design, semi-active suspension system, commercial car, LQR

Introduction

Semi-active suspensions are automotive systems that control the damping force of the shock absorber in response to input from the continuously varying road surfaces. The design of such systems involves multiple and often conflicting criteria. Furthermore, the performance of these systems greatly impacted by the variations in their physical parameters. As a result, their design should be conducted in multi-objective settings that ensure a robust behavior.

Several studies have been reported about the multi-objective optimal design of semi-active suspension systems. For example, a multi-objective design of a semi-active car suspension system with magnetorheological dampers is conducted by (Crews, Mattson, & Bucker, 2011). Two conflicting objective functions are selected: thermal performance and absorbed power. The control limitations are implemented on the control inputs which are taken as design variables. Skyhook, feedback linearization, and sliding mode controls are implemented and their performances are compared. The optimization is performed by a multi-objective genetic algorithm to achieve the final Pareto frontier. The results showed that this approach was not able to accommodate real-time control solutions that would operate with the Pareto frontier. While (Anaya-Martinez, et al., 2020) evaluated a semi-active suspension system with a magneto-rheological suspension system in electric vehicles. The main goal was to find a compromise solution between better road grip and ride comfortability. A switched reluctance motor was attached to the unsprung mass for engaging the spring and damper to reduce vibration. The simulation results obtained from pseudo bode plots showed that the skyhook and Mix one sensor controller provide the best enhancement in terms of the design goals. In another work, an optimal design of a semi-active suspension system is conducted by genetic algorithms (Koulocheris, Papaioannou, & Chrysos, 2017). The root-mean-square acceleration and the median of front and rear wheel travel were determined as cost functions. The damping coefficient of the suspension system and spring stiffness of the tire were chosen as the setup parameters. The

skyhook two-state damper control, skyhook linear approximation damper control, power-driven damper control, acceleration driven damper control, and mixed skyhook acceleration driving control were used as control algorithms.

The study provided detailed comparisons among these techniques. Also (Khadr & Romdhane, 2016) employed a continuous skyhook control and modified skyhook control in the optimal control of a semi-active suspension system in two-wheeled vehicles. The root-mean-square of vertical acceleration of the chassis and the wheel dynamic load were selected as design targets to achieve the best comfort and the drive safety. The front and rear damping coefficients of skyhook dampers were defined as design parameters. The NSGA-II was used to solve the optimization problem. The multi objective optimization results exhibited that both control laws guarantee the highest comfort and dive safety. In another study, a linear quadratic regulator (LQR) and mixed H_2/H_∞ optimization control were employed in the optimal design of a semi-active suspension system (Ye & Zheng, 2019). The vehicle vertical acceleration, suspension travel, and wheel dynamic load were defined as control objectives. Numerical simulations were carried out by MATLAB/Simulink and compared with those of the passive suspension system. The performance of the closed-loop system under these control strategies showed improved comfort and road handling. However, (lazaro, Villegas, Ruiz, & Aldana, 2019) developed fuzzy and PID controls for a semi-active suspension system with magnetorheological damper. Passengers' comfort, ride handling, and ground contact of the wheel were selected as control objectives. The results demonstrated that both control strategies were proven to be effective, but the fuzzy controller was the most acceptable in terms of comfortability. A Model predictive control (MPC) algorithm for vibration attenuation was applied on a semi-active suspension system with a magneto-rheological (MR) damper (Mai, Yoon, Choi, & Kim, 2020). The vertical sprung mass acceleration and sprung mass displacement were defined as design objectives. Both bump and random excitations were used as inputs to test the performance of the controlled system numerically and experimentally. The results demonstrated that the algorithm successfully achieved the highest ride comfort and road handling for the semi-active suspension system with MR dampers. An optimal control design of a semi-active suspension system consisting of a magnetorheological shock absorber under both skyhook and linear quadratic regulators was presented by (Majdoub, et al., 2018). The chassis vertical travel and drive comfort were used as cost functions. The viscous damping coefficients and wheel stiffnesses were defined as design parameters. The numerical simulations obtained by MATLAB/ Simulink manifested that the performance of the suspension system under the linear quadratic regulator was better than that of the skyhook controller. In another work, an energy efficient look-ahead cruise controller integrated with adaptive semi-active suspension system was presented for a utility commercial vehicle by (Basargan, Mihály, Gáspár , & Sename, 2020). The optimization criteria were to minimize the horizontal control force and the velocity limits for achieving the occupant's comfort and ride stability. The tire stiffness, damping rate of the shock absorber, and spring stiffness were used as design variables. The multi-criteria optimization problem was solved by the look-ahead estimation algorithm based on global positioning system. The results showed an improved vehicle adaptability based on the variations of the vehicle velocity.

Based on the above literature review, designing a semi-active suspension system by considering more than one objective and uncertainties in its mechanical components, which undergo variations due to either manufacturing errors or operation, has not been investigated. Their values will certainly impact the performance of the suspension system. Robust multi-objective optimization technique, which aims to reduce the sensitivity of the design objectives to the uncertainties in the model parameters, is proposed to fill the above research gap in the literature.

Robust Multi-Objective Optimization

Multi-objective optimization problems (MOPs) have received much attention recently because of their enormous applications. A MOP can be stated as follows:

$$\min_{\boldsymbol{K}\in\boldsymbol{Q}}\{\boldsymbol{F}(\boldsymbol{K})\}. \quad (1)$$

Similarly, robust multi-objective optimization problems (RMOPs) can be stated as:

$$\min_{\boldsymbol{K}\in\boldsymbol{Q}}\{\boldsymbol{F}^{eff}(\boldsymbol{K})\}, \quad (2)$$

Where the superscript *eff* denotes the mean effective of the objective space. Thus, **F** and $\boldsymbol{F^{eff}}$ are the maps that respectively consist of the objective functions $f_i: Q \to \mathbb{R}^1$ and the mean effective objective functions $f_i^{eff}: Q \to \mathbb{R}^1$ under consideration.

$$\boldsymbol{F}: \boldsymbol{Q} \to \mathbb{R}^k, \boldsymbol{F}(\boldsymbol{K}) = [f_1(\boldsymbol{K}), \quad \ldots, \quad f_k(\boldsymbol{K})] \tag{3}$$

$$\boldsymbol{F^{eff}}: \boldsymbol{Q} \to \mathbb{R}^k, \boldsymbol{F^{eff}}(\boldsymbol{K}) = \left[{f_1}^{eff}(\boldsymbol{K}), \quad \ldots, \quad {f_k}^{eff}(\boldsymbol{K})\right] \tag{4}$$

$\boldsymbol{K} \in \boldsymbol{Q}$ is a q-dimensional vector of design parameters. The domain $\boldsymbol{Q} \in \mathbb{R}^q$ can in general be expressed by inequality and equality constraints or their mean effective values (for RMOPs). For MOPs, **Q** is given by

$$\boldsymbol{Q} = \begin{Bmatrix} \boldsymbol{K} \in \mathbb{R}^q | g_i(\boldsymbol{K}) \leq 0, i = 1, \ldots, l \\ and \quad h_i(\boldsymbol{K}) = 0, j = 1, \ldots, n \end{Bmatrix}. \tag{5}$$

Similarly, for RMOPs, **Q** reads

$$\boldsymbol{Q} = \begin{Bmatrix} \boldsymbol{K} \in \mathbb{R}^q | g_i^{eff}(\boldsymbol{K}) \leq 0, i = 1, \ldots, l \\ and \quad h_i^{eff}(\boldsymbol{K}) = 0, j = 1, \ldots, n \end{Bmatrix}. \tag{6}$$

Here, *l* and *n* denote respectively the number of the inequality and equality constraints. Mathematically, f_i^{eff} is defined as:

$$f_i^{eff} = \frac{1}{|\boldsymbol{B_\delta}(\boldsymbol{K})|} \int_{\boldsymbol{y} \in \boldsymbol{B_\delta}(\boldsymbol{K})} f_i(\boldsymbol{y})\, d\boldsymbol{y}. \tag{7}$$

Where **δ** is the uncertainty vector with *q* elements, $\mathbf{B}_\delta(\mathbf{K})$ is the hyper-volume generated by randomly varying **K** using **δ** as follows: [**K** −**δ**, **K** +**δ**]). Thus, a finite set of r solutions are randomly created within the perturbed range of **K** and then used to evaluate $\boldsymbol{F^{eff}}$(Deb, K.; Gupta, H., 2006).

RMOPs are more attractive than MOPs since they aim at finding less sensitive trade-offs among the design objectives. The solution of MOPs and RMOPs forms a set known as the Pareto set and the corresponding set of the objective values is called the Pareto front. The dominancy concept (Marler & Arora, 2004) is used to find the optimal solution. The MOPs and RMOPs are solved using multi-objective optimization algorithms. These methods can be classified into scalarization, Pareto, and non-scalarization non-Pareto methods (sardahi, 2016).

The scalarization methods such as the weighted sum, goal attainment, and lexicographic approach require transformation of the MOP into a single optimization problem (SOP) (Pareto, 1971)), normally by using coefficients, exponents, constraint limits, etc.; and then methods for single objective optimization are utilized to search for a single solution. Computationally, these methods find a unique solution efficiently and converge quickly. However, these methods cannot discover the global Pareto solution for non-convex problems. Also, it is not always clear for the designer how to choose the weighting factors (Hernández, et al., 2013).

Unlike the scalarization methods, the Pareto methods do not aggregate the elements of the objectives into a single fitness function. They keep the objectives separate all the time during the optimization process. Therefore, they can handle all conflicting design criteria independently and compromise them simultaneously. The Pareto methods provide decision-makers with a set of solutions such that every solution in the set expresses a different trade-off among the functions in the objective space. Then, the decision-maker can select any point from this set. Compared to the scalarization approaches, the Pareto methods can successfully find the optimal or near optimal solution set, but they are computationally more expensive. Examples of evolutionary algorithms that fall under this category are the MOGA (Multiple Objective Genetic Algorithm), PSO (Particle Swarm Optimization), NSGA-II (Non-dominated Sorting Genetic Algorithm), SPEA2 (Strength Pareto Evolutionary Algorithm), and NPGA-II (Niched Pareto Genetic Algorithm). Mainstream evolutionary algorithms for MOPs include NSGA-II, multi-objective particle swarm optimization (MOPSO) and strength Pareto evolutionary algorithm (SPEA). Deterministic methods such as set oriented methods with subdivision techniques, and multi-objective algorithms based on the simple cell mapping (SCM) can be also used to find the solution set (sardahi, 2016).

The ϵ−constraint method and the VEGA (Vector Evaluated Genetic Algorithm) are examples of the non-scalarization non-Pareto methods. In the ϵ−constraint method, one of the cost functions is selected to be optimized and the rest of the functions in the objective space are converted into constraints by setting an upper bound to each of them. The VEGA works almost in the same way as the single objective genetic algorithm, but with a modified selection process. A comprehensive survey of the methods used for solving MOPs can be found in (Marler & Arora, 2004), and (Tian, Cheng, Zhang, & Jin, 2017).

Semi-active suspension systems can be optimally designed by using any one of these techniques. The optimization problems of these systems are complex and nonconvex, therefore evolutionary algorithms are the methods of choice (Woźniak, 2010). They outperform classical direct and gradient based methods which suffer from the following problems when dealing with non-linear, non-convex, and complex problems: 1) the convergence to an optimal solution depends on the initial solution supplied by the user, and 2) most algorithms tend to get stuck at a local or sub-optimal solution. On other side, evolutionary algorithms are computationally expensive (Hu, Huang, & Wang, 2003). However, this cost can be justified if a more accurate solution is desired and the optimization is conducted offline. The most widely used multi-objective optimization algorithm is the NSGA-II (Sardahi & Boker, 2018). It yields a better Pareto front as compared to other algorithms (Gadhvi, Savsani, & Patel, 2016). Therefore, in this paper, we use the NSGA-II to solve the robust multi-objective problems. For numerical simulations, a mathematical model of a quarter passenger car is used.

Passenger Car Model

A quarter car model of a passenger car implementing a semi-active suspension system is shown in Figure 1. In the model, the passenger is modelled as a two-degree-of-freedom system by splitting the passenger's body mass into two parts: m_t and m_p and they are connected by an assumed spring k_t and damper c_t. The cushion's elastic properties are modeled as an equivalent spring k_c and damper c_c which couple m_p to the sprung mass m_s. The suspension system is modeled as a spring with constant k_s, and damper with coefficient c_s. The control force, $u(t)$, is calculated by the LQR algorithm assuming that the vertical displacement of the sprung and un-sprung masses (z_s and z_u) and their first derivatives are available for feedback. The vertical displacement of the head and thorax z_t, pelvis and cushion z_p, and thier velocities are assumed to be unavialable and thuse not used in the control design. The driver and seat models are considered to add a more realsitic scenario to the design of the suspension system. In the figure, z_r denotes the road excitation. By the first principle modelling, the dynamics of the system reads:

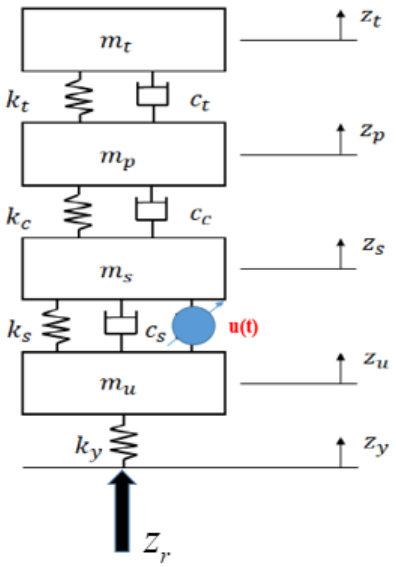

Figure 1. Passenger Car Model with Semi Active Suspension System

$$m_t\ddot{z}_t = -c_t(\dot{z}_t - \dot{z}_p) - k_t(z_t - z_p) \quad (8)$$

$$m_p\ddot{z}_p = c_t(\dot{z}_t - \dot{z}_p) + k_t(z_t - z_p) - c_c(\dot{z}_p - \dot{z}_s) - k_c(z_p - z_s) \quad (9)$$

$$m_s\ddot{z}_s = c_c(\dot{z}_p - \dot{z}_s) + k_c(z_p - z_s) - c_s(\dot{z}_s - \dot{z}_u) - k_s(z_s - z_u) + u(t) \quad (10)$$

$$m_u\ddot{z}_u = c_s(\dot{z}_s - \dot{z}_u) + k_s(z_s - z_u) - k_y(z_u - z_s) - k_y(z_u - z_r) - u(t) \quad (11)$$

If the seat and the driver are not included, the model reads

$$m_s\ddot{z}_s = -c_s(\dot{z}_s - \dot{z}_u) - k_s(z_s - z_u) + u(t) \quad (12)$$

$$m_u\ddot{z}_u = c_s(\dot{z}_s - \dot{z}_u) + k_s(z_s - z_u) - k_y(z_u - z_s) - k_y(z_u - z_r) - u(t) \quad (13)$$

Equations (8-11) will be used in the numerical calculations of the objective functions after coumputing the control gain vector using the state-space model of Equations (12-13) which is given by

$$\dot{\boldsymbol{x}}(t) = \boldsymbol{A}\boldsymbol{x}(t) + \boldsymbol{B}_y z_r(t) + \boldsymbol{B}_u u(t), \quad (14)$$

where, $\boldsymbol{x}(t) = [z_s \quad z_u \quad \dot{z}_s \quad \dot{z}_u]$ is the state vector, **A** is the dynamic matrix, $\mathbf{B_y}$ is the input vector that shows the influence of road excitation on the system dynamics, and $\mathbf{B_u}$ is the control input vector.

Control Design

The control force, $u(t)$, can be designed in different ways. One of the popular method methods in classical optimal control is the LQR. The control force is given by,

$$u(t) = -\boldsymbol{K}_f\boldsymbol{x}(t) \quad (15)$$

The optimal state feedback control gain matrix $\mathbf{K_f}$ can be obtained by minimizing the following quadratic cost function:

$$J = \int_0^\infty (\boldsymbol{x}^T(t)\boldsymbol{S}\boldsymbol{x}(t) + u^T(t)Ru(t))dt. \quad (16)$$

Where, $\mathbf{S} = \mathbf{S}^{\mathrm{T}}$ is a positive semidefinite matrix that penalizes the departure of system states from their equilibria, and $R = R^T$ is a positive definite matrix that penalizes the control force. Using Lagrange multiplier-based optimization method, the optimal $\mathbf{K_f}$ is given by

$$\boldsymbol{K}_f = R^{-1}\boldsymbol{B}_u\boldsymbol{P} \quad (17)$$

The matrix $\boldsymbol{P} \in \mathbb{R}^{4\times4}$ can be calculated by solving the following Algebraic Riccati Equation (ARE):

$$\boldsymbol{A}^T\boldsymbol{P} + \boldsymbol{P}\boldsymbol{A} - \boldsymbol{S} - \boldsymbol{P}\boldsymbol{B}_u R^{-1}\boldsymbol{B}_u^T\boldsymbol{P} = 0 \quad (18)$$

Inspecting Equations (17) and (18), we can notice that the choice of **S** and R will greatly affect the performance of the controlled system. Thus, these weighting matrices need to be tuned. Traditionally, **S** and R are chosen based on the expert of the control system designer and tweaked iteratively to achieve the design requirements. Arbitrary settings of **S** and R may result in non-optimal performance. Many works have been proposed about establishing systematic approaches for calculating **S** and R. For example, Bryson developed a method for selecting these matrices, but his method shows only how the initial values should be selected and the designer still needs to tune the elements of **S** and R for optimal performance (Bryson, 2018). Other examples can be found in (Oral, Çetin, & and Uyar, 2010) and (El Hajjaji & Ouladsine, 2001). Therein, analytical methods for selecting **S** and R for second order and third-order systems were developed. So, these techniques cannot be used to calculate **S** and R for the control algorithm applied to the semi-active suspension system because of its dimensionality. Hence, we suggest a numerical approach to tackle this problem.

Robust multi objective optimization optimal design (RMOD)

We consider the RMOD for the semi-active suspension system. The design vector reads

$$\boldsymbol{K} = \left[k_s, c_s, k_y, S_1, \ldots, S_4, R\right]. \quad (19)$$

The variables k_s, c_s and k_y are the passive elements of the suspension system shown in Figure 1. The variables $S_1,\ldots,S_4$ are on the diagonal of **S**, and R is the control force weighting factor. The constraints on the design parameter space are given by

$$\boldsymbol{Q} = \left\{ \begin{array}{l} \boldsymbol{K} \in \mathbb{R}^8 | S_1,\ldots,S_4 \in [0,100], \\ R \in [1.0\times10^{-6},100], \\ k_y \in [95,285]\times10^3, \\ k_s \in [11750,35250], \\ c_s \in [350,1050] \end{array} \right\}. \tag{20}$$

The upper bounds of S_1... $S4$, and R are chosen so that the penalties on the departures of the states from their desired positions and control utilization are high. The upper and lower bounds of k_s, c_s and k_y were chosen according to the work presented in (Nagarkar, Patil, & Patil, 2016).

The tire stiffness depends on the inflation pressure and road temperature. It also varies from one manufacturer to another. Furthermore, k_y changes due to wear while it is in service. To account for these factors, k_y is allowed to undergo 10% variations $\left(k_y \pm \delta_{k_y} k_y\right)$ (Loyer & Jézéquel, 2009), where $\delta_{k_y} = 10\%$. The spring and damping coefficients of the suspension system will degrade during the service due to aging and wear and their values will decrease over time. To simulate these variations, k_s and c_s uncertainties are defined as follows

$$\delta_{k_s} = \delta_{c_s} \in [-25,0]\%. \tag{21}$$

The design parameters defined in Equation (19) with their constraints given in Equation (20) and by considering $\delta_{k_y}, \delta_{k_s}, \delta_{c_s}$ are tuned to concurrently satisfy three objectives:

$$\min_{\boldsymbol{K}\in\boldsymbol{Q}} \left\{ {S_D}^{eff}(\boldsymbol{K}), {T_D}^{eff}(\boldsymbol{K}), {a_H}^{eff}(\boldsymbol{K}) \right\}, \tag{22}$$

Where, S_D^{eff}, T_D^{eff} and a_H^{eff} are respectively the mean-effective values of the suspension stroke $(S_D = z_s - z_u)$, the tire deflection $(T_D = z_u - z_r)$, and head acceleration $(a_H = \ddot{z}_t)$. Mathematically, they are given by

$$S_D^{eff}(\boldsymbol{K}) = \frac{1}{|\boldsymbol{B}_{\boldsymbol{\delta}}(\boldsymbol{K})|} \int_{\boldsymbol{y}\in\boldsymbol{B}_{\boldsymbol{\delta}}(\boldsymbol{K})} S_D^{RMS}(\boldsymbol{y}) d\boldsymbol{y}. \tag{23}$$

$$T_D^{eff} = \frac{1}{|\boldsymbol{B}_{\boldsymbol{\delta}}(\boldsymbol{K})|} \int_{\boldsymbol{y}\in\boldsymbol{B}_{\boldsymbol{\delta}}(\boldsymbol{K})} T_D^{RMS}(\boldsymbol{y}) d\boldsymbol{y}. \tag{24}$$

$$a_H^{eff} = \frac{1}{|\boldsymbol{B}_{\boldsymbol{\delta}}(\boldsymbol{K})|} \int_{\boldsymbol{y}\in\boldsymbol{B}_{\boldsymbol{\delta}}(\boldsymbol{K})} a_H^{RMS}(\boldsymbol{y}) d\boldsymbol{y}. \tag{25}$$

Here, **y** is one of the perturbed and randomly created solutions that makes the hyper-volume $\mathbf{B}_\delta(\mathbf{K})$ (See the Robust Multi-Objective Optimization Section for more details). The superscript *RMS* denotes the root-mean-square operation. The RMS of S_D, T_D and a_H read

$$S_D^{RMS} = \left[\frac{1}{T}\int_0^T S_D^2(t)dt\right]^{\frac{1}{2}}, \tag{26}$$

$$T_D^{RMS} = \left[\frac{1}{T}\int_0^T T_D^2(t)dt\right]^{\frac{1}{2}}, \tag{27}$$

$$a_H^{RMS} = \left[\frac{1}{T}\int_0^T a_H^2(t)dt\right]^{\frac{1}{2}}. \tag{28}$$

Here, T represents the duration of measurement. It is obvious that the environmental and operational variabilities of k_y, k_s and c_s can be simulated by considering their uncertainties $\delta_{k_y}, \delta_{k_s}$, and δ_{c_s}. But the question is: can the variations in the other system parameters, namely $m_t, m_p, k_t, c_t, k_c, c_c$, and m_s alter the design objectives? To answer this question, sensitivity analysis should be conducted.

Global Sensitivity Analysis (GSA)

Global sensitivity analysis (GSA) is conducted by the Fourier Amplitude Sensitivity Test (FAST), which is one of the most popular uncertainty and sensitivity analysis techniques. GSA allows for the sensitivity analysis to be examined over the complete solution domain rather than a local approximation around the nominal value. The FAST algorithm is a computationally efficient method which based on Monte Carlo sampling. The algorithm employs a peridic sampling method and a Fourier transformation to calculate the variance of the input parameters so that the most influential parameters may be identified. The reader can refer to the work by (El-Sharkawy, 2014) for more details about this method.

In this paper, the uncertainties of m_t, m_p, k_t, and$c_t$are set to$\pm 20\%$ to simulate the fact that different drivers with different dynamics may drive the same car. Since their values decrease over time, the seat spring $k_c$and damper c_c are allowed to vary between $[k_c - 0.1k_c, k_c]$and $[c_c - 0.1c_c, c_c]$, respectively. The sprung mass $m_s$fluctuates due to the variation of car occupants and luggage. Following the work of Loyer and Jézéquel (Loyer & Jézéquel, 2009), m_s is assumed to undergo 10% variations $(m_s \pm 0.1m_s)$. The sensitivity indices of the seven parameters are demonstrated for the *RMS* of the three design objectives.

Furthermore, the sensitivities of the objectives are evaluated at different levels of the control force. Figures 2-7 show the sensitivity indices when $u(t)$ is large (LQR algorithm's settings:$R = 1.0 \times 10^{-6}, S_1 = S_2 = S_3 = S_4 = 100$) and it is small (LQR settings: $R = 100, S_1 = S_2 = S_3 = S_4 = 0$). It is evident from these figures that $S_D^{RMS}$and $T_D^{RMS}$are mainly affected by the variations of m_s, m_t and; but$m_s$is recording the highest impact. The other four parameters $k_t, c_t, k_c$and$c_c$have almost no effect on $S_D^{RMS}$and T_D^{RMS}.

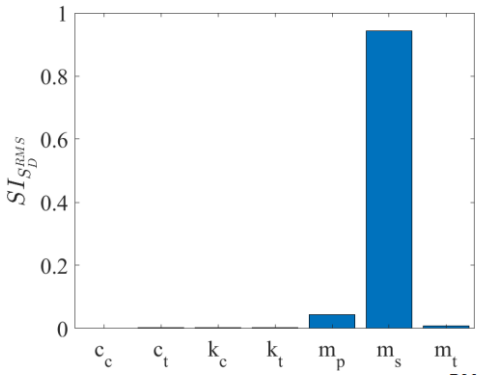

Figure 2. Sensitivity Indices of the Input Paramters on $S_D^{RMS}$when $u(t)$ is large.

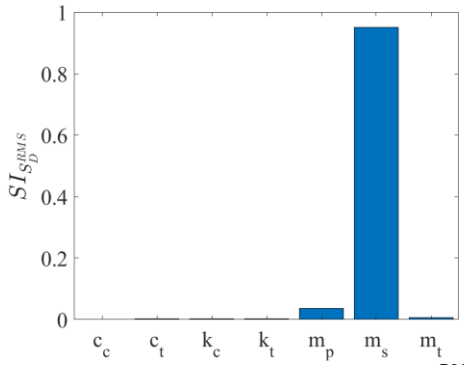

Figure 3. Sensitivity Indices of the Input Paramters on $S_D^{RMS}$when $u(t)$ is small.

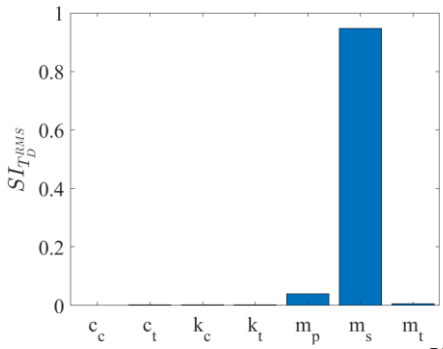

Figure 4. Sensitivity indices of the input paramters on $T_D^{RMS}$when $u(t)$ is large.

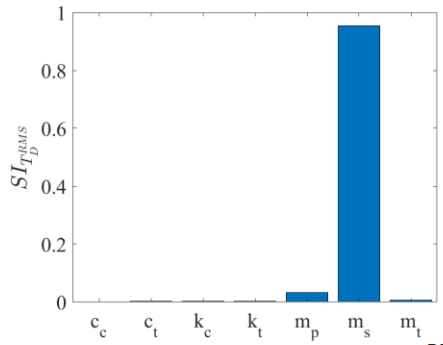

Figure 5. Sensitivity indices of the input paramters on $T_D^{RMS}$when $u(t)$ is small.

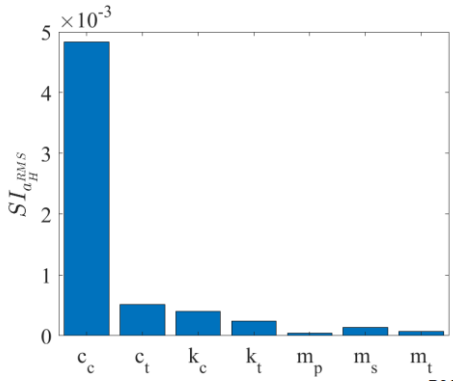

Figure 6. Sensitivity indices of the input paramters on $a_H^{RMS}$when $u(t)$ is large.

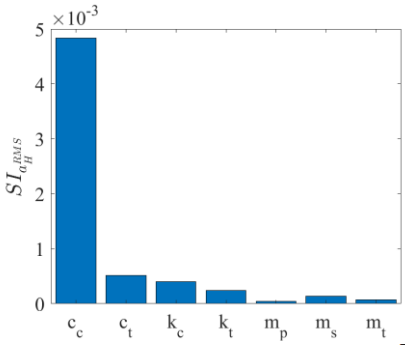

Figure 7. Sensitivity indices of the input paramters on $a_H^{RMS}$when $u(t)$ is small.

In a similar fashion, the sensitivity indices of the model variables are calculated for a_H^{RMS}at large $u(t)$ and small $u(t)$ and are depicted in Figures 6 and 7, respectively. The figures demonstrate that $a_H^{RMS}$is insensitive to these elements since the sensitivity indices are extremely small.

To sum up, it is obvious that the deviations in $m_s$will certainly influence the values of two cost functions from the selected three design objectives. As a result, $m_s$is varied during the optimization to find less sensitive and robust solution to the optimization problem at hand.

Optimization Setup

To solve the RMOP at hand , the NSGA-II is used. During the optimization, the population size is set to 50 and the maximum number of function evaluations is set 1000. For the robust solution, a finite set of 20 solutions are randomly created within the neighborhood of the nominal values of k_y, k_s, c_s, and m_s. Then, the mean effective values of the objective functions are calculated. The quarter-car model is simulated with MATLAB using ode15s for 10 seconds with a step size of 10 millisecond. During the numerical simulation, the nominal value of $m_s$is set to *290 kg*. According to (Gündoğdu, 2007) and (Kuznetsov, Mammadov, Sultan, & Hajilarov, 2011), other parameters can be set to: $m_p = 46.43kg$, $m_t = 18.57kg$, $k_t = 45005.3N/m$, $c_t = 1360$ $N.s/m$,$k_c = 10000N/m$, and $c_c = 900$ $N.s/m$. Following the work of Shirahatti and his colleagues (Shirahatti, Prasad, Panzade, & Kulkarni, 2008), the road profilez_r (see Equation 29) is chosen as a sinusoidal shape having two successive depressions of depth$h = 0.05m$, and length $\lambda = 20m$ when the vehicle velocity $v = 20m/s$.

$$z_r = \begin{cases} \frac{h}{2}\left(1 - cos\left(\frac{2\pi v}{\lambda}t\right)\right), & 0 \le t \le \frac{2\lambda}{v} \\ 0, & otherwise \end{cases} \quad (29)$$

Under these conditions, the robust multi-objective optimization problem is solved and its solution in terms of the robust Pareto front and set are obtained.

Results and Discussion

Projections of the robust Pareto front are shown in Figures 8 and 9. The robust trade-offs between the effective-mean of the head acceleration and that of the suspension deflection are depicted in Figure 8, while those between the suspension deflection and tire deflection are plotted in Figure 9. Both projections exhibit competing relationships among the design objectives. For instance, by inspecting Figure (8), we notice thata_H^{eff} decreases as S_D^{eff} goes up. Similarly, T_D^{eff} goes down asS_D^{eff} increases. The competing nature of these objectives stresses out the fact that these objectives need to be handled in multi-objective settings. Projections of the corresponding Pareto sets are graphed in Figure 10. The optimal passive components (c_s versus k_s and the color is mapped to the value of k_y) are depicted in Figure 10-a. The subplot shows that higher values of c_s are associated with higher levels of k_y. While the active design parameters of the suspension systems are plotted in 10-b and 10-c. The color in these subfigures is mapped to the level of the control penalizing factor, R. These subplots demonstrate that the weighting elements of the LQR algorithm fall within their feasible ranges and different optimal solutions can be found by adjusting them optimally. In order to show the robustness of these solutions, time-domain profiles of the suspension deflection, tire deflection, and head acceleration at random point from the Pareto set are discussed next.

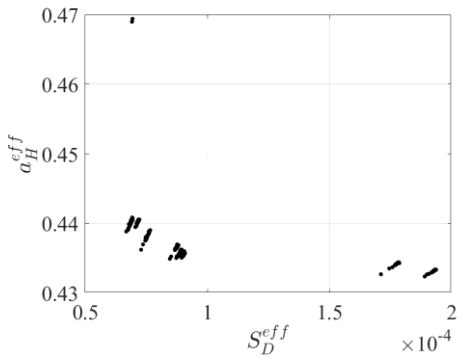

Figure 8. Robust Optimal Pareto Front of the Mean-effective Value of the Head Acceleration versus Suspension Deflection

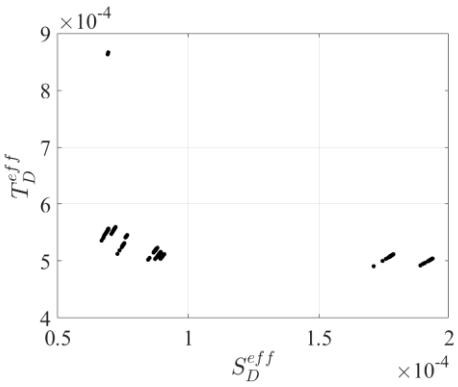

Figure 9. Robust Optimal Pareto Front of the Mean-effective Value Tire Deflection versus Suspension Deflection

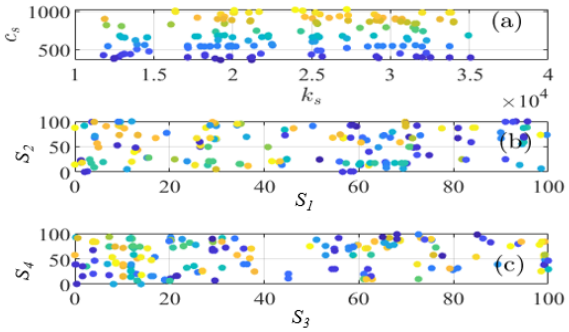

Figure 10. Robust Pareto Set (a) the color is mapped to the value k_y (b) & (c) the color is mapped to the value of the control weighting factor R

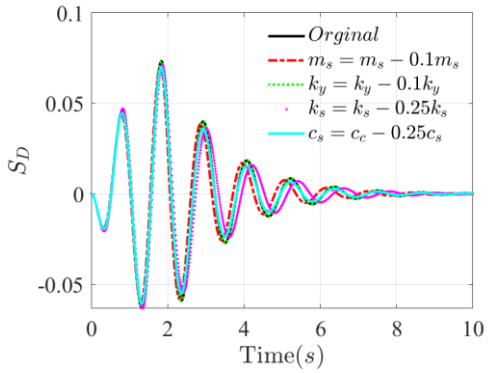

Figure 11. Time Response of Suspension Deflection at the Lower Levels of the Suspension Passive Elements

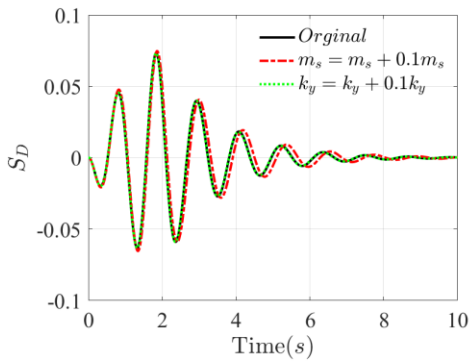

Figure 12. Time Response of Suspension Deflection at the Upper Levels of the Suspension Passive Elements

The profiles of the suspension deflection at the lower and upper values of $m_s, k_y, k_s$and $c_s$are shown in Figures 11 and 12. The responses manifest little deviations from the ideal response (labeled original in the legend). The sprung spring and damping constants seem to have more impact on the$S_D$profile as compared to the other parameters. This is expected since they tie up the sprung mass to the tire. The variables$m_s$and $k_y$have less impact on$S_D$as shown in these figures. Inspecting the profiles of the tire deflection shown in Figures 13 and 14 at different conditions, we notice that the response is insensitive to variations in $m_s$and c_s, and slightly deviate from its ideal profile when$k_s$and$k_y$are degraded. Similarly, the passenger head acceleration (see Figures 15 and 16) show little corrupt from its ideal response when the passive elements of the suspension are perturbed. This emphasizes the importance of the robust design of semi-active suspension systems to ensure that the performance criteria do not largely deviate after implementation.

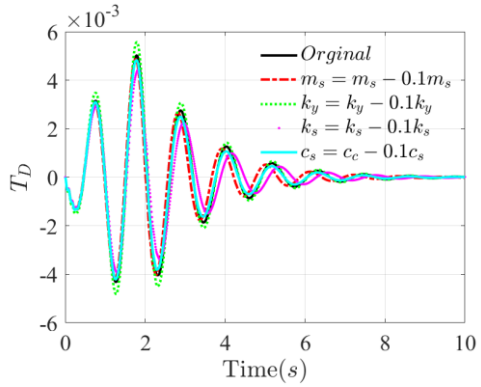

Figure 13. Time Response of Tire Deflection at the Lower Levels of the Suspension Passive Elements

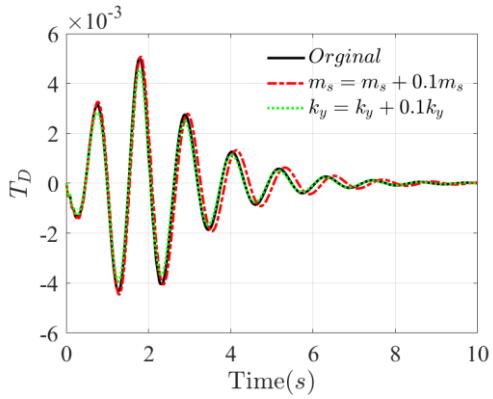

Figure 14. Time Response of Tire Deflection at the Upper Levels of the Suspension Passive Elements

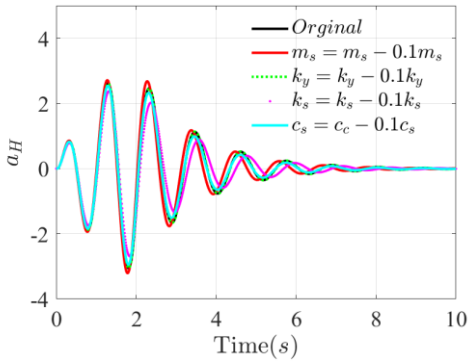

Figure 15. Time Response of Head Acceleration at the Lower Levels Of the Suspension Passive Elements

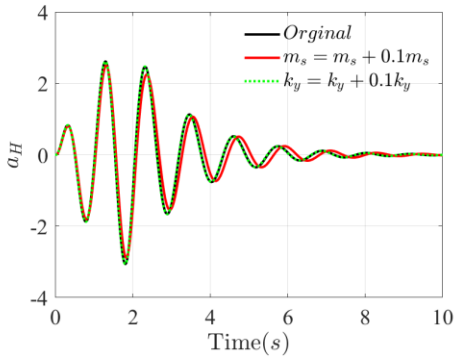

Figure 16. Time Response of Head Acceleration at the Upper Levels of the Suspension Passive Elements

Conclusion

We have studied the robust multi-objective design of a semi-active suspension system used in a commercial car. The optimization problem with 8 design parameters and 3 objective functions is solved by the NSGA-II algorithm. The sprung mass of the vehicle, tire stiffness, and suspension stiffness and damping constants are assumed to be uncertain and varied during the optimization to account for their variability. The robust Pareto set, and front are obtained. The Pareto set includes multiple design options from which the decision-maker can choose to implement. Time profiles of the design objectives show that the robust multi-objective design algorithm is very effective and guarantees less sensitivity to the suspension passive components.

References

Anaya-Martinez, M., Lozoya-Santos, J.-d.-J., Félix-Herrán, L., Tudon-Martinez, J.-C., Ramirez-Mendoza, R.-A., & Morales-Menendez, R. (2020). Control of Automotive Semi-Active MR Suspensions for In-Wheel Electric Vehicles. *journal of applied sciences*, 10.

Basargan, H., Mihály, A., Gáspár , P., & Sename, O. (2020). Integrated multi-criteria velocity and semi-active suspension control. *2020 28th Mediterranean Conference on Control and Automation (MED).* Saint-Raphaël, France: Institute of Electrical and Electronics Engineers .

Bryson, A. E. (2018). *Applied optimal control: optimization, estimation and control* . Routledge.

Crews, J., Mattson, M. G., & Bucker, G. D. (2011). Multi-objective control optimization for semi-active vehicle suspensions. *Journal of Sound and Vibration*, 5502–5516.

Deb, K., & Gupta, H. (2006). Introducing robustness in multi-objective optimization. *Evolutionary computation*, 463- 494.

El Hajjaji, A., & Ouladsine, M. (2001). Modeling and nonlinear control of magnetic levitation systems. *IEEE Transactions on industrial Electronics, 48*(4), 831-838.

El-Sharkawy, A. (2014). Sensitivity and Uncertainty Analysis in Computational Thermal Models. *SAE Technical Paper*. doi:https://doi.org/10.4271/2014-01-0656

Gadhvi, B., Savsani, V., & Patel, V. (2016). Multi-objective optimization of vehicle passive suspension system using NSGA-II, SPEA2 and PESA-II. *Procedia Technology*, 361-368.

Gündoğdu, Ö. (2007). Optimal seat and suspension design for a quarter car with driver model using genetic algorithms,. *International Journal of Industrial Ergonomics*, 327-332.

Hernández, C., Naranjani, Y., Sardahi, Y., Liang, W., Schütze, O., & Sun, J.-Q. (2013). Simple cell mapping method for multi-objective optimal feedback control design. *International Journal of Dynamics and Control*, 1(3), 231-238.

Hu, X., Huang, Z., & Wang, Z. (2003). Hybridization of the multi-objective evolutionary algorithms and the gradient-based algorithms. *In The 2003 Congress on Evolutionary Computation, 2003. CEC'03*, Vol. 2, pp. 870-877.

Khadr, A., & Romdhane, L. (2016). Design and optimization of a semi-active suspension system for a two-wheeled vehicle using a full multibody model. *Journal of Multi body dynamics*, 1-17.

Koulocheris, D., Papaioannou, G., & Chrysos , E. (2017). A comparison of optimal semi-active suspension systems regarding vehicle ride comfort. *Materials Science and Engineering.* Athens, Greece: Institute of Physics.

Kuznetsov, A., Mammadov, M., Sultan, I., & Hajilarov, E. (2011). Optimization of improved suspension system with inerter device of the quartercar model in vibration analysis. *Archive of Applied Mechanics*, 1427-1437.

lazaro, J. M., Villegas, H. E., Ruiz, B., & Aldana, A. (2019). Control Design Strategies for Semi-Active Suspension System. *International Mechanical Engineering Congress and Exposition.* Salt Lake City, Utah: American Society of Mechanical Engineers.

Loyer, B., & Jézéquel, L. (2009). *Robust design of a passive linear quarter car suspension system using a multi-objective evolutionary algorithm and analytical robustness indexes.* London: Taylor and Francis.

Mai, V. N., Yoon, D.-S., Choi, S.-B., & Kim, G.-W. (2020). Explicit model predictive control of semi-active suspension systems with magneto-rheological dampers subject. *Journal of Intelligent Material Systems*, 1-14.

Majdoub, E. K., Ouadi, H., Belbounaguia, N., Kheddioui, E., Souhail, R., & Ammari1, O. (2018). Optimal Control of Semi-Active Suspension Quarter Car Employing Magnetorheological Damper and Dahl Model. *Renewable Energies, Power Systems & Green Inclusive Economy (REPS-GIE).* Casablanca, Morocco: Institute of Electrical and Electronics Engineers.

Marler, R. T., & Arora, J. S. (2004). Survey of multi-objective optimization methods for engineering. *Structural and multidisciplinary optimization, 26*(6), 369-395.

Nagarkar, M. P., Patil, G. J., & Patil, R. N. (2016). *Optimization of nonlinear quarter car suspension–seat–driver mode* (Vol. 7).

Oral, Ö., Çetin, L., & and Uyar, E. (2010). A Novel Method on Selection of Q And R Matrices In The Theory Of Optimal Control. *International Journal of Systems Control, 1*(2).

Pareto, V. (1971). Manual of political economy.

sardahi, Y. (2016). Multi-objective optimal design of control systems. *Doctoral dissertation, UC Merced*.

Sardahi, Y., & Boker, A. (2018). Multi-objective optimal design of four-parameter PID controls. *Dynamic Systems and Control Conference.* Atlanta, Georgia: ASME.

Shirahatti, A., Prasad, P. S., Panzade, P., & Kulkarni, M. M. (2008). Optimal design of passenger car suspension for ride and road holding. *Journal of the Brazilian Society of Mechanical Sciences and Engineering, 30*(1), 66-76.

Tian, Y., Cheng, R., Zhang, X., & Jin, Y. (2017). PlatEMO: A MATLAB platform for evolutionary multi-objective optimization [educational forum]. *IEEE Computational Intelligence Magazine, 12*(4), 73-87.

Woźniak, P. (2010). Multi-objective control systems design with criteria reduction. *In Asia-Pacific Conference on Simulated Evolution and Learning*, 583-587.

Ye, H., & Zheng, L. (2019). Comparative study of semi-active suspension based on LQR control and H2/H∞ multi-objective control. *Chinese Automation Congress (CAC).* Hangzhou: Institute of Electrical and Electronics Engineers.

-